disk: JGII; doc: sim.study global carbon cycle

A SIMULATION STUDY FOR THE GLOBAL CARBON CYCLE, INCLUDING MAN'S IMPACT ON THE BIOSPHERE

J. Goudriaan and P. Ketner

1) Department of Theoretical Production Ecology, Agricultural University, Bornsesteeg 65, 6708 PD Wageningen, the Netherlands.

2) Department of Vegetation science, Plant ecology and Weed science, Agricultural University, De Dreijen 11, 6703 BC Wageningen, the Netherlands.

Keywords: CO_2, simulation, global carbon cycle

ABSTRACT

The simulation model accounts for four major compartments in the global carbon cycle: atmosphere, ocean, terrestrial biosphere and fossil carbon reservoir. The ocean is further compartmentalized into a high and a low latitude surface layer, and into 10 deep sea strata. The oceanic carbon fluxes are caused by massflow of descending and upwelling water, by precipitation of organic material and by diffusion exchange.

The biosphere is horizontally subdivided into six ecosystems and vertically into leaves, branches, stemwood, roots, litter, young humus and stable soil carbon. Deforestation, slash and burn agriculture, rangeland burning and shifts in land use have been included. The atmosphere is treated as one well mixed reservoir. Fossil fuel consumption is simulated with historic data, and with IIASA scenario's for the future. Using the low IIASA scenario an atmospheric CO_2 concentration of 431 ppmv is simulated for 2030 AD. A sensitivity analysis shows the importance of different parameters and of human behaviour. Notwithstanding the large size of the biosphere fluxes, the atmospheric CO_2 concentration in the next century will be predominantly determined by the growth rate of fossil fuel consumption.

1. Introduction

A numerical simulation model is the most convenient and practicable tool for a quantitative integration of knowledge in multicompartment system with many non-linear relations. This description certainly applies to the global carbon cycle.

In the past several models for the carbon cycle have been developed (Bolin et al., 1979; Oeschger et al., 1975; Pearman, 1980). In the model presented here special attention is given to the impact of human interference in the biosphere through deforestation and changes in land use, without loosing the important interaction with the oceans. Therefore both biosphere and ocean need considerable spatial and functional resolution. The importance of fossil fuel consumption must be evaluated by using different scenario's.

The equations for the fluxes between the reservoirs are written as regular differential equations. Solving these differential equations by analytic-mathematical methods either requires highly involved methods (Siré et al., 1981) or depends on rigorous simplifications (MacIntyre, 1980). Here the differential equations are solved by numerical integration using CSMP[1]. This simulation language enables computer formulations that are close to the original differential equations.

2. Fossil fuel consumption

The rate of fossil consumption, F_{fa}, is a function of time only (Figure 1), and not influenced by remaining reserves. Still, the size of the fossil fuel reservoir is simulated to check if the total carbon simulated is constant. The differential equation for the fossil fuel reservoir N_f is

$$\frac{dN_f}{dt} = - F_{fa} \qquad (1)$$

The time course of F_{fa} (Figure 1) is a fit to data of Rotty (1980), and from 1980 to 2030 extrapolations have been used from a high and low scenario of IIASA (Schipper, 1981).

3. Atmosphere

The atmosphere is not compartmentalized because rapid turbulent transfer ensures that CO_2 concentration variations between different parts of the world remain below 4 ppmv (Fraser et al., 1980).

1) Listings of the model can be obtained from the senior author.

The model is initialized with a guessed situation in 1780. The atmospheric CO_2 concentration is estimated to have been 285 ppmv at that time, or about 600 Gt C. The relation between CO_2 concentration and total atmospheric carbon in Gt C is:

$$C_a = 0.4754\ N_a \tag{2}$$

The atmosphere receives carbon by fossil fuel combustion and exchanges carbon with both the biosphere and the ocean. The net annual carbon gain of the biosphere, if no human interference occurred, is called the total net ecosystem production TNEP. Presumably, about two centuries ago this rate just balanced the rate of carbon release induced by human disturbance HDIST. The same applies to the oceanic fluxes. The organic material precipitating into the deep sea (F_g) causes a concentration gradient that drives upward fluxes. As a result the net diffusion exchange F_{ma} between the mixing layers and the atmosphere was almost zero.

The resulting equation for the carbon content of the atmosphere is

$$\frac{dN_a}{dt} = F_{fa} + F_{ma} + \text{HDIST} - \text{TNEP} \tag{3}$$

The driving force of fossil fuel combustion F_{fa} increases the atmospheric carbon content N_a. Then an imbalance develops in the net diffusion flux F_{ma}, and part of the flux F_{fa} is absorbed in the ocean. Dependent on the response of the biosphere to increasing CO_2 also an imbalance in the pair HDIST - TNEP may develop. On the other hand, growing population pressure independently raises HDIST.

4. Ocean

The compartmentalization of the ocean is given in Figure 2. The two surface layers have been distinguished to represent roughly the latitude dependence of mixing in the ocean water. For the same purpose Viecelli et al. (1981) used three latitudinal zones. The layer in the lower latitudes is rather thin (75 m) and receives upwelling water from the deep sea with a relatively high carbon content. To maintain the water balance the same volume of water flows to the thicker surface layer (400 m) at higher latitudes. From this layer the massflow descends in the arctic seas and it is equally distributed over the nine deep sea layers, so that the resulting slow upwelling water movement increases from bottom to top. At the top the upwelling enters the thin layer in the lower latitude zones. The total flow rate $\emptyset$ of this circulation is estimated at $75 \times 10^6\ m^3\ s^{-1}$ (Gordon, 1971) or $2.3 \times 10^{15}\ m^3\ y^{-1}$, resulting in a turnover time of the upper layer of 6 years.

A third layer of 325 m thickness fills the gap between the thin, low latitude layer and the first layer of the deep sea, which is divided into 9 equal layers of 3400/9 m each.

In addition to the massflow all layers exchange water by turbulent mixing with an average eddy-diffusion coefficient of 4000 $m^2\ y^{-1}$ (Oeschger et al. 1975). The diffusion and the massflow term together form the flux $FO_{i,j}$ from ocean layer i to ocean layer j:

$$FO_{i,2} = - \phi * C_2/9 \qquad 5 \leq i \leq 12 \tag{4a}$$

$$FO_{i,i-1} = + \phi * C_i * (13-i)/9 + (C_i - C_{i-1}) * D * A/T_i \qquad 5 \leq i \leq 12 \tag{4b}$$

$$FO_{2,1} = - \phi * C_1 \tag{4c}$$

$$FO_{4,2} = - \phi * C_2/9 + (C_4 - C_2) * D * A * 0.5/(0.5 * T_2 + 0.5 * T_4) \tag{4d}$$

$$FO_{4,3} = + \phi * C_4 + (C_4 - C_3) * D * A * 0.5/(0.5 * T_4 + 0.5 * T_3) \tag{4e}$$

$$FO_{3,1} = + \phi * C_3 + (C_3 - C_1) * D * A * 0.5/(0.5 * T_3 + 0.5 * T_1) \tag{4f}$$

where the symbols are:

C_i	carbon concentration in layer i	
D	diffusion coefficient	($4000\ m^2\ y^{-1}$)
A	ocean area	($360 * 10^{12} m^2$)
T_i	layer thickness	
ϕ	massflow of water	($2.3 * 10^{15}\ m^3\ y^{-1}$)

The factor 13-i in the massflow term represents the increase in upwelling from bottom to top.

The matrix $FO_{i,j}$ is anti-symmetric with diagonal zero. All elements other than defined in Eqn 4 are zero.

The net carbon gain of a layer consists of all fluxes FO to that layer and of its share of the gravitational flux F_g:

$$\frac{dO_i}{dt} = \sum_{j=1}^{12} FO_{j,i} + F_{g,i} \tag{5}$$

with $F_{g,i} = -F_g/2$ for $i = 1,2$ (5a)

$$F_{g,i} = F_g/9 \quad \text{for } 4 \leq i \leq 12 \tag{5b}$$

$$F_{g,i} = 0 \quad \text{for } i = 3 \tag{5c}$$

The concentration C_i is calculated as

$$C_i = O_i/V_i \tag{6}$$

where the volume V_i is calculated as the product of layer thickness and area.

These exchange equations are all linear, because water masses transport carbon as a passive admixture. At the interface between ocean and atmosphere the situation is different because a shift in chemical equilibria is involved.

Their effect can be summarized by the buffer factor (Bolin et al., 1979):

$$\zeta \frac{dO_{eq}}{O_{eq}} = \frac{dATM}{ATM} \tag{7}$$

The buffer factor ζ is about 10, but depends on the atmospheric CO_2 partial pressure concentration as given in Figure 3 (derived from Bacastow and Keeling, 1973). In the model ζ is independent from temperature, but the starting position of the equilibrium carbon content for the thin and warm surface layer is lower. With a temperature of 20°C it is initialized at 23.7 g C m^{-3} (in equilibrium with 285 ppmv) instead of 26.6 g C m^{-3} for the thick and cold layer. If the atmospheric concentration does not change too much, all equations can be made linear. We can represent the oceans as proportional absorbers but with a carbon content that is ζ (about 10) times smaller than the real one. The effective total oceanic carbon content is thus more than 5 times as large as the atmospheric one, so that the ultimate remanent fraction of carbon in the atmosphere is about 1/(5+1) (17%).

At present this value is much higher ($\approx$ 58%) because the deep sea is not participating fast enough. In the numerical model the equilibrium contents of the surface layers O_1 and O_2 can be simulated by Eqn 8. The difference between the actual and the equilibrium contents drives the net diffusion flux to the atmosphere:

$$F_{1ma} = (O_1 - O_{1,eq})/\tau_{1a} \quad (8a)$$

$$F_{2ma} = (O_2 - O_{2,eq})/\tau_{2a} \quad (8b)$$

This equation is derived from the assumption that the carbon concentration of water at the sea surface is in equilibrium with the atmospheric CO_2 concentration. With the diffusion equation the relaxation times τ_{1a} and τ_{2a} can be expressed as $T^2/(2D)$, yielding values of about 1 and 20 years resp. The exchange rate at the atmosphere-sea interface is much faster (Broecker and Peng, 1974), and therefore not rate-limiting, so that the above assumption is justified.

In an equilibrium situation that presumably existed before the industrial era the net diffusion and mass flow balanced the gravitational precipitation F_g. The precipitation flux gives rise to an increase in carbon concentration with depth, which maintains an opposite diffusion flux. It is known from measurements that the carbon concentration rises from about 26 g m^{-3} at the surface to over 29 g m^{-3} at large depths. The simulation model generates such an increase with a gravitational flux F_g equal to about 8 Gt C y^{-1} (Figure 4). In comparison with the estimated net primary production of the oceans of 45 Gt C y^{-1} (De Vooys, 1979) this is a large flux. No response of the gravitational flux to CO_2 is present in the model, because biological production in the oceans is not carbon-limited.

The profile as given in Figure 4 is in equilibrium with a gravitational flux of 8 Gt C y^{-1}, and is used as the initial status of the oceanic part of the model. In the initial segment of the CSMP model it is generated by an iterative method.

4.2 Model results without biosphere

The model developed so far simulates the global carbon cycle without interference of the terrestrial biosphere. It does so with fairly good results (Figure 5) the simulated CO_2 concentration in 1980 is 334 vpm. However, the simulated remanent fraction is 0.68, higher than the actual 0.58. It simulates that out of the 162 Gt C injected into the atmosphere since 1780, 103 Gt C have remained there (average 64% remanent), 4.5 Gt C moved to the thin surface layer, 17 Gt C to the thicker high latitude layer and 37 Gt C to the deep sea.

The compartmentalization of the deep sea ensures a sufficiently fine grid to solve numerically the diffusion exchange. As Oeschger et al. (1975) pointed out, a lumped deep sea box underestimates absorption of admixtures on time scales smaller than some decades. In our model the ocean has absorbed about 10 Gt C less in the

year 1980 if the deep sea strata are lumped into one box. On the other hand, an even finer resolution than 10 strata is not worthwhile.

For a separate study on ocean behaviour a further extrapolation was made to 2250 A.D. with a logistic type curve, peaking in 2050 with a maximum of 14 GT C y^{-1} and a total cumulative injection of 1700 Gt C (Viecelli et al., 1981) (Figure 6).

$$F_{fa} = 4*14*E/(1 + E)^2 \quad (9a)$$

$$E = \exp(R*(TIME - 2050)) \quad (9b)$$

$$R = 4*14/1700 \quad (9c)$$

5. Terrestrial biosphere

Although the ocean model alone gives reasonable results, the biosphere must be included to represent the effects of deforestation and of other human activities which cause a CO_2-output of the same magnitude as the fossil fuel combustion. The biospheric section of the model explains how this large flux is largely recirculated.

5.1 Without land transfer between ecosystems

In this model 6 different land ecosystems are distinguished with a general structure of carbon flow as given in Figure 7.

The driving input of the ecosystem is the net primary production NPP, made up of the difference between the gross annual assimilation of carbon on one hand and respirational loss on the other (Larcher, 1980; Cooper, 1975). Later we will present arguments that the NPP is influenced by atmospheric CO_2, and is independent of biomass. The NPP is partitioned among the four main components: leaves, branches, stems and roots according to fixed distribution coefficients p_{jk}. j denotes the ecosystem number (1-6) and k the plant component number (1-4), so that

$$\sum_{k=1}^{4} p_{jk} = 1 \quad (10)$$

The outflow from each components in Figure 7 is equal to its content divided by its average life-span. The aboveground biomass components then flow to the litterpool, the roots flow to the humuspool. The resulting differential equations for the change of the biomass components B are

$$\frac{dB_{jk}}{dt} = p_{jk} * NPP_j - \frac{B_{jk}}{\tau(B_{jk})} \tag{11}$$

For litter (L) the differential equation is

$$\frac{dL_j}{dt} = \sum_{k=1}^{3} \frac{B_{jk}}{\tau(B_{jk})} - \frac{L_j}{\tau(L_j)} \tag{12}$$

Litter has a turnover time of only 1 or 2 years, and when it decays, only a fraction λ_j is transferred to the humuspool. The rest is released by respiration to the atmosphere. Humus (H) decays much slower, and a fraction ϕ_j enters a pool of relatively stable carbon (K) that contains recalcitrant humus, charcoal and other forms of elementary carbon (Kortleven, 1963). This pool decays very slowly. No permanent sink (as fossil carbon) is added. If it exists its dynamics are too slow to be important on the time scale of centuries.

$$\frac{dH_j}{dt} = \lambda_j \left[\frac{L_j}{\tau(L_j)} + \frac{B_{j4}}{\tau(B_{j4})} \right] - \frac{H_j}{\tau(H_j)} \tag{13}$$

$$\frac{dK_j}{dt} = \frac{\phi_j H_j}{\tau(H_j)} - \frac{K_j}{\tau(K_j)} \tag{14}$$

The net ecosystem production per biome NEP_j is equal to the net primary production NPP_j, diminished with the carbon released upon the decay of litter, roots, humus and charcoal:

$$NEP_j = NPP_j - \left[\frac{L_j}{\tau(L_j)} + \frac{B_{j4}}{\tau(B_{j4})} \right] * (1-\lambda_j) - \frac{H_j(1-\phi_j)}{\tau(H_j)} - \frac{K_j}{\tau(K_j)} \tag{15}$$

The total net ecosystem production TNEP of the terrestrial biosphere as used in Equation 3, consists of the sum of the NEP_j's of the six ecosystems.

The units of the pools and fluxes are Gt C and Gt C y^{-1} resp. The corresponding surface densities are found by dividing them by the ecosystem area.

The parameters used in these equations are given in Table 1. These figures are educated guesses, but agree with a vast number of experimental data from agricultural and ecological research. For instance in grassland twice as much of the assimilates flow to the roots than in agricultural land. The vegetation of human area is considered as being a sparse temperate forest, so that the parameters in Table 1 are practically the same. Humus lives much shorter in tropical forest than elsewhere. These parameters determine the ratio's of the carbon content of the different components in the equilibrium situation.

Table 1

Parameters of the flow through the terrestrial biosphere

		Tropical Forest	Temperate Forest	Grass-land	Agricultural area	Human area	Tundra and semi-desert
Partitioning	Leaf	0.3	0.3	0.6	0.8	0.3	0.5
	Branch	0.2	0.2	0.	0.	0.2	0.1
	Stem	0.3	0.3	0.	0.	0.3	0.1
	Root	0.2	0.2	0.4	0.2	0.2	0.3
Life span	Leaf	1	2	1	1	1	1
	Branch	10	10	10	10	10	10
	Stem	30	60	50	50	50	50
	Root	10	10	1	1	10	2
	Litter	1	2	2	1	2	2
	Humus	10	50	40	25	50	50
	Charcoal	500	500	500	500	500	500
Humification factor λ		0.4	0.6	0.6	0.2	0.5	0.6
Carbonization factor ϕ upon humus decomposition		0.05	0.05	0.05	0.05	0.05	0.05

Carbonization factor (ε_k) upon burning of leaves is 0.05, of branches 0.1, of stems 0.2 and of litter (ε_L) is 0.1

The steady state solution of the Equations 11-14 is:

$$B_{jk} = NPP_j * p_{jk} * \tau(B_{jk}) \quad (16)$$

$$L_j = NPP_j * (1 - p_{j4}) * \tau(L_j) \quad (17)$$

$$H_j = NPP_j * \lambda_j * \tau(H_j) \quad (18)$$

$$K_j = NPP_j * \lambda_j * \phi_j * \tau(K_j) \quad (19)$$

Data of Ajtay et al. (1979) were used to calculate the areal net primary productivities (in g C m^{-2} y^{-1}) and present total areas (in 10^{12} m^2) (Table 2). We grouped tropical forests, forest plantations, shrub dominated savanna's and chaparral into our class of 'Tropical Forest', and temperate and boreal forests and woodlands into our class of 'Temperate forest'. We omitted extreme deserts and perpetual ice because of their negligible contribution to the fluxes.

Table 2

Areal net primary productivities, areas (1980), total NPP and actual biomass
(From Ajtay et al., 1979)

	σ(NPP) g C m^{-2} y^{-1}	Area 10^{12} m^2	NPP Gt C y^{-1}	Biomass GtC
Tropical Forest	770	36.1	27.8	324.7
Temperate Forest	510	17.0	8.7	186.8
Grassland	570	18.8	10.7	15.1
Agricultural land	430	17.4	7.5	3.0
Human area	100	2.0	0.2	1.4
Tundra and semi-desert	70	29.7	2.1	13.3
		121	57.0	544.3

Using these data, and with Eqns 16-19, the contents of the different biomass components, of litter, humus and charcoal can also be calculated (Table 3).

Table 3

Calculated equilibrium contents of biospheric components in Gt G without cutting and burning but present areas of ecosystems

	Tropical Forest	Temperate Forest	Grass-land	Agricultu-ral area	Human area	Tundra and semi-desert	Total
Leaves	8.34	5.2	6.43	5.98	0.06	1.04	27.1
Branches	55.6	17.3	0.	0.	0.4	2.08	75.4
Stems	250.2	156.1	0.	0.	3.	10.4	419.7
Roots	55.6	17.3	4.29	1.5	0.4	1.25	80.3 +
Biomass	369.7	195.91	10.72	7.48	3.86	14.8	602.5
Litter	22.23	13.87	12.86	5.99	0.32	2.94	58.2
Humus	111.19	260.1	257.18	37.41	5.0	63.	733.9
Charcoal	277.97	130.05	160.74	37.41	5.0	31.5	642.7

The total biomass (603) computed in this way is higher than the actual biomass (544), but no allowance has been made yet for cutting and burning.

Another interesting result of these calculations is the leaf biomass. When it is divided by the area of the ecosystem we obtain the leaf biomass density and find about 300 g C m^{-2} for forest, grassland and agricultural area, and ten times less for human area and tundra/semi-desert. Typically leaves contain about 20-40 g C m^{-2} with reference to their own area, so that annually about 8-15 m^2 of leaf area is produced per m^2 of ground area. Because a Leaf Area Index (LAI) of 3 m^2 (leaf) per m^2 (ground) is sufficient for complete light interception, the net primary production is saturated with respect to biomass. Only in human area and in the tundra/semi-desert ecosystems is the vegetation sparse and may a positive feedback between NPP and biomass exist. In the most important ecosystems no coupling is necessary so that the simple, linear differential equations can be used with solutions of the type of Eqns 16-19.

5.2 Cutting, burning and shifting cultivation

Human interference has large effects on the size of the pools of carbon in the ecosystems. Forests are cut down and burnt, and also grassland and agricultural land after harvest is frequently burnt. From the data provided by Seiler and

Crutzen (1980) the annual area of tropical forest cut down for shifting cultivation can be estimated as about 15 Mha ($0.15*10^{12}$ m²). Of both agricultural land and grassland annually about 400 Mha (4×10^{12} m²) is burnt, or about a quarter of the total area. Cutting in temperate forests is much less sizeable, and amount to about 2 Mha y^{-1}.

The carbon of biomass and litter is not entirely channeled to the atmosphere, but a fraction ε_k (Table 1) is converted to long lasting charcoal. This fraction is 0.05 for leaves, 0.1 for branches and litter and 0.2 for stems (Seiler and Crutzen, 1980). Moreover, 0.5 of the stems remains as unburnt wood on the fields. From then on this fraction is treated as humus, because it has a similar turnover time. Consequently, the fraction that goes directly to the atmosphere (burning efficiency) is 0.95 for leaves and litter, 0.9 for branches and only 0.3 for stems.

Burning has two opposing effects in the carbon cycle. It certainly means a release of large amounts of CO_2 (source-effect), but it also effectuates a drain of carbon to long lasting charcoal (sink-effect). Because of burning the carbon contents of soils, especially of agricultural and grassland soils, are 20 to 40% higher than without burning. Humus and biomass on the other hand are decreased.

Regrowth occurs immediately after burning, because pioneer vegetation soon establishes. Therefore there is no effect of biomass present on the net primary production. The same value of NPP will drive the chain of delays as depicted in Figure 7, and restore the contents of the pools.

The intensity of shifting cultivation and burning are related to human population size, but this relation is less than proportional, because of increasing urbanization. As a reasonable estimate the area annually affected is proportional to the square root of the population, as if shifting cultivation and burning in agriculture occur at the fringe of a growing circle of population. With an annual growth rate of the population of 1.5% per year, the population size 200 years ago was only 5% of the present one. If the square root relationship holds, burning and shifting cultivation had an intensity of 22% of the present rate. This number is used for initialization of the carbon contents of the biospheric pools at the start of the simulation 200 years ago.

5.3 Land transfer

Any area shift is destructive for the aboveground biomass and litter, which in the model are treated in the same way as shifting cultivation. Below ground biomass (roots) die and are transferred to the humuspool. Humus and charcoal are not

released but enter the pool of the ecosystem that replaces them. They may consequently adopt a different lifetime.

An ecosystem may loose surface area at one location, but gain at another. Land exchange between the ecosystems can be represented by a time dependent exchange matrix a_{ij}, denoting the gross annual transfer of land from ecosystem j to ecosystem i.

Shifting cultivation and burning within an ecosystem can mathematically be represented by the diagonal of the transfer matrix (a_{jj}) (Table 4).

It should be noted that this matrix represents the gross annual transfers. Therefore it does not contain negative numbers and is not anti-symmetric (like matrix FO_{ij} for the ocean fluxes).

Table 4
Transfer matrix of area between ecosystems (Mha y^{-1}) in 1980 and their present total area.

To \ From	Tropical forest	Temperate forest	Grass-land	Agricultural land	Human area	Desert and tundra
Tropical forest	15	0	0	0	0	0
Temperate forest	0	2	0	0	0	0
Grassland	6	1	400	0	0	0
Agricultural area	6	0	0	400	0	2
Human area	0.5	0.5	1	1	0	0
Desert and tundra	0	0	0	0	0	0
Present area (1980)	3610	1705	1880	1745	200	2970
Initial area (1780)	4400	1800	1500	1300	10	3100

We used data of Seiler and Crutzen (1980) to make estimates for the values in this matrix. We had to extrapolate several regional figures to a global scale so that the reliability of these numbers is not high. The figures on the diagonal of this matrix are the least certain, because they are more difficult to assess than true transfer rates. Our figures for annual burning rate of forest and grassland are on the low side, but of agricultural land on the high side of what Seiler and Crutzen (1980) mention. In a sensitivity analysis we could show that a halving of the figures on the diagonal axis is much less influential than a halving of the transfer rates (Table 7). Grassland receives 6 Mha y^{-1} from tropical forest, mainly in Latin America, and about 1 from temperate forest. Agricultural area is increased at the expense of tropical forest and of semi-desert (irrigation).

Much has been written and said about desertification (U.N. Conference, 1977; Eckholm, 1976), the transition of agricultural land and of grassland to desert. It is difficult to find sound and well documented data on this process. Much of what is called desertification is indistinguishable from the large natural annual variation (Breman et al., 1982). Climatic changes are certainly not responsable for the apparent desertification, but rather soil degradation, erosion and over-grazing. These sort of changes hardly affect the net primary production, so that a shift in the model to the desert type area is not appropriate. What might occur is release of CO_2 from soil carbon, but in the regions where it is important the quantities of soil carbon are low anyway causing only a small loss.

Human area increases slowly, but mainly at the expense of grassland and agricultural land.

We assume that the land transfer rates outside the diagonal grow proportional to population (growing with 1.5% y^{-1}), but that burning and shifting cultivation which are represented by the diagonal, grow with the square root of population. The used initial areas in 1780 are chosen so that the simulated present area is in good agreement with the assessments of Ajtay et al. (1979).

The differential equations 11-14 must now be extended:

$$\frac{d\,B_{jk}}{dt} = p_{jk} * NPP - \frac{B_{jk}}{\tau(B_{jk})} - \sigma(B_{jk}) \sum_{i=1}^{6} a_{ij} \qquad (20)$$

$$\frac{d\,L_j}{dt} = \sum_{k=1}^{3} \frac{B_{jk}}{\tau(B_{jk})} - \frac{L_j}{\tau(L_j)} - \sigma(L_j) \sum_{i=1}^{6} a_{ij} \qquad (21)$$

$$\frac{d\,H_j}{dt} = \lambda_j \left[\frac{L_j}{\tau(L_j)} + \frac{B_{j4}}{\tau(B_{j4})}\right] - \frac{H_j}{\tau(H_j)} - \sigma(H_j) \sum_{i=1}^{6} a_{ij} +$$

$$+ \sum_{i=1}^{6} a_{ji} \left[\sigma(H_i) + \lambda_j\, \sigma(B_{i4}) + 0.5\, \sigma(B_{i3})\right] \qquad (22)$$

$$\frac{d\,K_j}{dt} = \frac{\phi_j H_j}{\tau(H_j)} - \frac{K_j}{\tau(K_j)} - \sigma(K_j) \sum_{i=1}^{6} a_{ij} +$$

$$+ \sum_{i=1}^{6} a_{ji} \left[\sigma(K_i) + \sum_{k=1}^{3} \epsilon_k\, \sigma(B_{ik}) + \epsilon_L \sigma(L_i)\right] \qquad (23)$$

The area A_j of ecosystem j changes as well:

$$\frac{dA_j}{dt} = \sum_{i=1}^{6} (a_{ji} - a_{ij}) \qquad (24)$$

The calculation of the net ecosystem production NEP_j (Eqn 15) is not changed. However, whereas it tends to be zero in a stable ecosystem, it is permanently positive when human disturbance is continually present. The carbon flux released due to human disturbance HDIST can be calculated as:

$$HDIST = \sum_{j=1}^{6} \sum_{i=1}^{6} a_{ij} \left[\sum_{k=1}^{3} (1-\varepsilon_k)\, \sigma(B_{jk}) - 0.5\ \sigma(B_{i3}) + (1-\lambda_j)\ \sigma(B_{i4}) + (1-\varepsilon_L)\ \sigma(L_i) \right] \qquad (25)$$

This flux enters the net rate of change of the carbon content of the atmosphere (Equation 1).

5.4 Stimulation of growth by CO_2

A simple way to represent the CO_2 effect is the stimulation of the net primary productivity according to a logarithmic increase. Although this curve lacks physiological significance on a single leaf basis, it is a convenient one parameter equation to represent the response of a complex system (Gifford, 1980). According to this equation the surface density of the net primary productivity $\sigma(NPP)$ is related to the atmosheric CO_2 concentration as

$$\sigma(NPP) = \sigma(NPP_o)*(1 + \beta(\ln(C_a/C_{ao})) \qquad (26a)$$

or

$$\frac{d\sigma\ (NPP)}{dC_a} = \beta\ \sigma(NPP_o)/C_a \qquad (26b)$$

The biotic growth factor β gives the relative response to CO_2 near the present CO_2-concentration. The numerical value of β is ill-known, but still of great

importance. Direct experimental evidence from greenhouses shows, that it may vary from zero under phosphate limitation, via 0.3 under nitrogen limitation to 0.7 under optimal supply of nutrients (Goudriaan & de Ruiter, 1983). In natural ecosystems water or nutrients usually limit production. Water use efficiency is improved by CO_2 increase (Gifford, 1979; Louwerse, 1980; Goudriaan & van Laar, 1978). Therefore it may be possible that vegetation in semi-arid zones will proliferate and grow denser, because of the increased water use efficiency under higher CO_2. Like climatic change, this is a very gradual process and still below the detection threshold. Locally it is overshadowed by erosion and overgrazing, but it would be wrong to generalize these processes to a global desertification.

Also other indirect CO_2 effects not present in pot experiments and greenhouse studies, may exist such as stimulation of root growth and of microbial activity, whereby nutrient availability increases (Rosenberg, 1981). Simultaneously with rising CO_2 diffuse eutrofication with NO_x^- and NH_4^+ occurs to some extent.

For these reasons the overall CO_2 effect is probably larger than the directly measurable one. Gifford (1980) found that a biotic growth factor of 0.6 is required to reproduce the atmospheric trend; in this paper a value of 0.5 appears necessary to find the solid line in Figure 5. The difference between this value found by model calibration and the directly measurable value with an average of 0.2-0.3, can be viewed as a garbage can collecting the additional stimulating effects.

6. Results

The simulated pools and fluxes in 1980 A.D. have been represented with increasing resolution in the Figures 8 and 9. In these figures the area of the pools and the width of the fluxes are proportional to their sizes. The time course of these pools and of some fluxes is given in Table 5. The biospheric pools are a result of the driving net primary production, its partitioning, and the life-spans of the components. Both input parameters and simulated output (Table 6) are consistent with statistical data as given by Ajtay et al. (1979). For instance, temperate forest and grassland contain more than twice as much soil carbon per surface area than tropical forest and agricultural land.

In forests 30 percent of the NPP is allotted to the leaves. Still, leaf weight is only 2.5 percent of the total biomass in tropical forest and 2.9 percent in temperate forest because leaves live short in comparison to wood. Root weight is good for 16 percent in tropical forest, 9.3 percent in temperate forest, 40 percent in grassland and 20 percent in agricultural area, of the total biomass of the ecosystem.

In Fig. 9, the annual rates of change of the global totals of biomass, litter, humus and charcoal have been divided into fluxes caused by natural processes and those caused by human disturbance. For instance, the total net change of biomass is equal to -0.9 Gt C y^{-1}. This rate is the result of an input by NPP of 61.85 Gt C y^{-1}, subtracted with the natural fluxes 'litter fall' (42.62) and 'root death' (14.40), resulting in a net increase of 5.83 Gt C y^{-1} by natural processes. Human disturbance causes a biomass burning of 3.46 Gt C y^{-1}, a biomass carbonization of 0.60, an immediate stem and root decay on transferred land of 0.85, and a humification flux of the same stems and roots of 1.82 Gt C y^{-1}. The ultimate rate of change is -0.9 Gt C y^{-1} (5.83-6.73), which can also be composed according to ecosystem type (Table 7). This table shows that the sum of the annual increases by natural processes (calculated by Eqn 11-14), the total net ecosystem production (TNEP), is as high as 7.25 Gt C y^{-1}. This large number is caused by regrowth in response to prior human disturbance. Human disturbance tends to bring biomass and litter below their natural equilibrium, but humus and charcoal above it. Natural processes counteract these forces, so that the signs of the totals for aboveground and below-ground carbon in Table 7 alternate. Tundra/Semi-desert is the only model ecosystem in which the natural processes are independent of human disturbance, and only caused by the CO_2 effect. This ecosystem does loose land, so that the annual increases due to land transfer are negative. Human area on the contrary receives land, sothat it has a large positive flux due to human disturbance, consisting of import of humus and charcoal.

The large number of decimals in Table 7 must not be mistaken for a suggestion of accuracy, but is a reflection of the fact that many fluxes together almost cancel. The net positive uptake of the entire biosphere (0.33 Gt C y^{-1}) can be considered as a slight and temporary unbalance of large and opposed fluxes. For this reason a direct experimental verification of the net fluxes is practically impossible. Still, we can put some confidence in these calculations because they allow for the inherent feedback mechanism.

Another interesting analysis is the separation of the fluxes into a CO_2 effect and a human disturbance effect. The best way to obtain CO_2-effect is a comparison with the model results for a run with a zero biotic growth factor. The fluxes for the separate, but entire, ecosystems are given in Table 7 below the figures for the standard run. The comparison shows that the entire biosphere has become a source of CO_2 of 1.13 Gt C y^{-1}. The difference is caused by a decreased NEP, but slightly counteracted by decreased biomass in areas affected by human disturbance.

The stimulation of growth by CO_2 is the reason that the terrestrial biosphere as a whole is now a net sink for CO_2, even though a small one. In the past the situation was reversed and the biosphere was a source. According to the model the

turning point was 1967. This past source effect is still visible as an increased atmospheric CO_2 content but at present the rate of increase is less than in an ocean-only model (Figure 5). Because of this gradual shift of biospheric action from source to sink, the oceanic uptake averaged over the past 100 years have been a larger fraction (about 44%) of the fossil fuel injection than at present (about 35%). For the same reason the ocean has absorbed more carbon (78 Gt C) in that period of time than it would have done without biospheric action (58 Gt C), simulated with the ocean-only model.

7. Some other simulation models

Bacastow and Keeling (1973) developed an early model of the carbon cycle which contained both ocean and land biota. Because of the constraints of analytic solubility this model was kept simple. The ocean only contained two compartments, and the biosphere also. Fossil consumption grew at 4 percent per year. As we now know this rate was not maintained, so that the projections by this model are way too high.

Oeschger et al. (1975) developed a model which emphasis on the ocean. The biosphere was represented by one box with a delayed CO_2- response. The ocean was treated according to the box-diffusion method. This hybrid method gives a large improvement as compared to models with two or three well-mixed oceanic reservoirs. Oeschger used 14_C data to estimate the average diffusion coefficient in the ocean (4000 $m^2\ y^{-1}$).

Björkström (1979) used a model with many oceanic compartments. Geometrically our model for the ocean is very similar to his. In his model the deep sea exchanges water and carbon by massflow and a gravitational flux, but not by eddy-diffusion. The biosphere was divided into a phytomass and a soil carbon pool. A major conclusion of his work, which we support, is that the remanent fraction is quite stable. However, he used much lower figures for the carbon release from the biosphere (2 Gt C y^{-1} versus 7 in our model) and for the biotic growth factor (0.2 versus 0.5 in our model).

Pearman (1980) published a model for a stratified ocean. The biosphere appears as a constant source of 0.18 Gt C y^{-1}, obtained by calibration.

Gifford (1980) on the other hand only considered the biosphere. On basis of a subdivision into 9 ecosystems he found that the biosphere is able to store 1 Gt C y^{-1}, if the biotic growth factor is about 0.6. However, the effects of deforestation etc. were ignored.

Kohlmaier et al. (1981) published a model that is quite similar to ours in the structure of the biosphere. They calculated a net-emission of the biosphere of 2

Gt C y^{-1} caused by human disturbance. The major differences with our model are: an approximately doubled shifting cultivation, a much lower humus content in grassland soils, a much faster increase in agricultural land and no reservoir of long lasting charcoal.

Our model can be considered as a further expansion and integration of Björkström's and Kohlmaier's models.

8. Model projections, and discussion

The most important element of a projection of the future CO_2 concentration is the energy scenario. As a standard the low IIASA scenario is used (Figure 1) in which the carbon emission grows from 5.2 Gt C y^{-1} in 1975 to 8.9 Gt C y^{-1} in 2030. In this scenario the atmospheric CO_2 concentration will have reached 431 ppmv in 2030. However, if the high IIASA scenario is used, in which the annual C-combustion in 2030 equals 16.2 Gt C y^{-1}, the atmospheric CO_2 concentration will then be as high as 482 ppmv. If, on the other hand, a zero growth scenario would be followed in which the annual combustion remains constant at 5.2 Gt C y^{-1} the atmospheric CO_2 concentration in 2030 would be 404 ppmv.

It is useful to compare the range of these projections with the uncertainty as caused by poor knowledge of parameter values. Any uncertainty from such sources is additional to the variation caused by energy scenario's or other types of human behaviour.

The results of a sensitivity analysis are listed in Table 8. Some parameters have a surprisingly small influence on the model behaviour. The reason is the initialization procedure which ensures consistency of the initial size of the reservoirs and the parameter values. The most outspoken example is the absence of any effect of the gravitional flux of organic matter in the oceans on the dynamic behaviour of atmospheric CO_2. Certainly the shape of the concentration profile with depth is altered, but because it is a linear superposition the dynamic behaviour is not. To a lesser extent the same argument applies to the small effect of doubling the life-span of charcoal or of humus. The total stock is also doubled but its dynamics is hardly changed. In contrast, the life-span of biomass has a very large effect, apparently because the CO_2 release in deforestation is proportional to the standing biomass. Surprisingly the net effect of doubling the NPP is small, probably because both biomass, and with it the rate of CO_2 release in deforestation, as well as the stimulation of NPP by CO_2, are doubled.

The most important uncertainties are due to:

a) Diffusion coefficient in oceans
b) Life-span of biomass
c) Rate of deforestation and land reclamation
d) Biotic growth factor

To estimate the uncertainty by the year 2030 it is the difference between the 2030 and 1980 values in Table 8 that counts, because we know where we are standing now. Moreover it is not likely that we are more than 50% off in the estimates of the parameter values. If all uncertainties are independent, a reasonable estimate for the total uncertainty due to paremeter values is about 10 ppmv in the year 2030.

It is clear that the range in projected CO_2-concentrations due to energy scenario's is much larger than due to parameter uncertainties.

A remaining question is how effective some management of the biosphere could be, such as reforestation. Therefore a reforestation rate is introduced, starting with 10 Mha y^{-1} (0.1×10^{12} m^2 y^{-1}) in 1980 and increasing annually with 1.5%, the same as the population growth. This measure is superimposed on the regular human interference, such as represented by the matrix in Table 4. Its effect is a lowering of the atmospheric CO_2 concentration in 2030 by 10 ppmv, which is a very modest achievement in comparison to the size of the operation. It should be taken into account that the reforestation is supposedly taking place on grassland and agricultural land.

Another management policy could be to freeze the rate of deforestation, land reclamation, and rangeland burning at the rate of the year 1980. In that case the atmospheric CO_2 concentration in 2030 would be 12 ppmv lower than without the measure.

These simulation exercises demonstrate that the effect of environmental protection measures on the atmospheric CO_2 concentration is minor in comparison to the effect of changing energy consumption.

In this investigation of model sensitivity the parameters have not been changed during the simulation. If they do change in time they have much larger effects because the equilibrium value itself will drift away. A global warming, induced by CO_2, may tend to accelerate humus decay and thus the rate of CO_2 released at a stimulated rate. If the rate of decay is stimulated to the same extent as the net primary productivity ($\beta = 0.5$) the simulated 1980 CO_2 concentration is raised by 7 ppmv untill 347 ppmv. The size of this stimulation of decay is not unrealistic. It corresponds with a drop in humus turnover from 50 years in the temperate forests

in 1780 to 45 years at present, and to 33 years when the CO_2 concentration will be doubled. At that time the average temperature will be raised by 2-3 C (Manabe and Wetherald, 1975). Such changes in life-span are well possible, but hardly detectable by direct experimental methods.

Acknowledgements

The authors are grateful for the remarks, corrections and suggestions by Dr. Kohlmaier. Mr. Van Amersfoort typed the manuscript and Mr. Beekhof made the drawings.

Table 5

Simulated reservoirs and fluxes for a standard run.
Low IIASA scenario for fossil fuel combustion.

	1780	1880	1930	1980	2030
INJF	0.01	0.22	1.08	5.18	9.12
cumulative injection	0.	5.95	38.2	161.8	510.1
CO_2 conc.	285.	290.9	302.4	339.1	432.4
Reservoirs:					
ATMOSPHERE	599.5	611.9	636.0	714.2	909.5
BIOMASS	676.6	657.2	634.4	594.4	516.6
LITTER	57.0	55.0	53.7	52.7	52.2
HUMUS	686.8	683.9	685.5	700.7	757.4
CHARCOAL	734.6	743.4	756.0	778.3	819.8
OCEAN O_1	324.2	324.7	325.8	328.8	335.2
OCEAN O_2	1823.9	1826.4	1831.0	1843.6	1874.9
OCEAN $\sum_{i=3}^{12} O_i$	35804.0	35810.0	35823.0	35856.0	35951.0
Fluxes:					
NPP (total)	59.4	59.5	60.0	61.9	65.3
NEP (total)	1.58	3.02	4.47	7.25	11.32
HDIST	1.62	3.25	4.64	6.91	11.13
Remanent fraction	-	1.12	0.63	0.61	0.61

Table 6

Simulated distribution of biosperic components in 1980.

Pools in Gt C (10^{15} g)

	Tropical forest	Temperate forest	Grass-land	Agricultural land	Human area	Tundra and semi-desert
Leaves	9.00	5.63	5.73	5.27	0.064	1.13
Branches	57.22	18.38	0.	0.	0.37	2.22
Stems	239.47	154.77	0.	0.	1.80	10.81
Roots	57.22	18.38	3.82	1.32	0.37	1.35
Litter	22.59	14.39	8.01	4.28	0.27	3.12
Humus	117.58	268.00	205.18	35.21	10.12	64.60
Charcoal	312.36	136.86	195.36	87.67	14.72	31.31
Area (10^{12} m²)	36.08	17.04	18.80	17.43	2.00	29.73

Surface densities in kg C m^{-2}

Leaves	0.249	0.306	0.304	0.302	0.032	0.038
Branches	1.58	1.08	0.	0.	0.186	0.075
Stems	6.64	9.08	0.	0.	0.90	0.364
Roots	1.58	1.08	0.203	0.076	0.186	0.045
Litter	0.626	0.844	0.425	0.245	0.133	0.105
Humus	3.26	15.72	10.91	2.02	5.06	2.17
Charcoal	8.66	8.03	10.39	5.03	7.36	1.05

Table 7

Simulated rates of change of biospheric pools in 1980 A.D., by natural processes and due to human disturbance; composed per ecosystem type. Also the ecosystem totals, simulated for a biotic growth factor of zero are given. All rates are expressed in Gt C y^{-1}.

Annual change by natural processes	Tropical forest	Temperate forest	Grass-land	Agricultural land	Human area	Tundra/ semi-desert	Total
of Biomass	1.7561	0.3743	2.0846	1.5539	0.0427	0.0188	5.8304
of Litter	0.1149	0.0352	1.7288	0.9916	0.0044	0.0052	2.8801
of Humus	-0.4347	0.0618	-0.4327	-0.2888	-0.1174	0.0502	-1.1616
of Charcoal	-0.0368	-0.0057	-0.1342	-0.1049	-0.0193	0.0020	-0.2989 +
NEP	1.3995	0.4656	3.2465	2.1518	-0.0896	0.0762	7.2500
NEP (β=0)	0.6391	0.0638	2.7605	1.9179	-0.0960	0.	5.2853
Annual change due to burning within the ecosystem itself							
of Biomass	-1.5087	-0.2312	-2.0333	-1.5119	0.	0.	-5.2851
of Litter	-0.0939	-0.0169	-1.7043	-0.9820	0.	0.	-2.7971
of Humus	0.5929	0.1037	0.4879	0.0605	0.	0.	1.2450
of Charcoal	0.2341	0.0405	0.2314	0.1589	0.	0.	0.6649 +
	-0.7756	-0.1039	-3.0183	-2.2745	0.	0.	-6.1723
Annual change due to land transfer (with burning)							
of Biomass	-1.2573	-0.1735	-0.0051	-0.0038	0.	-0.0104	-1.4498
of Litter	-0.0783	-0.0127	-0.0042	-0.0025	0.	-0.0021	-0.0998
of Humus	-0.4074	-0.2358	0.5516	0.4407	0.2716	-0.0435	0.5772
of Charcoal	-1.0821	-0.1205	0.6097	0.5855	0.2565	-0.0211	0.2280 +
	-2.8251	-0.5425	1.1520	1.0199	0.5281	-0.0771	-0.744
-HDIST	-3.6007	-0.6464	-1.8663	-1.2546	0.5281	-0.0771	-6.9167
-HDIST (β=0)	-3.4556	-0.6264	-1.6673	-1.1057	0.5154	-0.0749	-6.4145 +
Net annual change in whole ecosystem	-2.2012	0.1662	1.3802	0.8972	0.4385	-0.0009	0.3333
same with β=0	-2.8165	-0.5626	1.0932	0.8122	0.4194	0.0749	-1.1292

Table 8

Change in the simulated atmospheric CO_2 concentration in ppmv in 1980 and in 2030 as result of a change in parameter values.

	1980	2030
Oceanic diffusion coefficent doubled (to 8000 m^2 y^{-1})	-4.87	-13.9
No descending water (Ø=0)	+3.7	+12.0
Carbonization factor halved	-0.3	-0.4
Carbonization factor (upon burning) halved	+4.4	+9.7
NPP doubled	+0.8	-6.4
Life-span biomass doubled	+16.5	+35.4
Life-span humus doubled	-0.9	-6.3
Life-span charcoal doubled	-0.5	-1.2
Litter humification factor halved	-0.1	+5.1
Biotic growth factor halved (to 0.25)	+7.6	+21.0
Deforestation and land reclamation rates halved	-5.3	-15.4
Rangeland burning and shifting cultivation rates halved	-3.0	-5.5
Relative decay rate of humus changes proportional with NPP	+7.1	+21.6
Changes in human behaviour		
Zero growth energy consumption in 1980	0.	-27.4
Zero growth population in 1980	0.	-11.9
Reforestation started in 1980 with 10 Mha y^{-1}, later proportional with population	0.	-10.
High IIASA energy scenario	+0.1	+50.9

List of symbols

A_j	Area of ecosystem j	Mha (10^{10} m²)
a_{ij}	Rate of transition of area from ecosystem j to ecosystem i	Mha y^{-1}
A_o	Area of the ocean (360×10^{12})	m²
B_{jk}	Carbon in ecosystem j in component k	Gt C
C_a	Atmospheric CO_2 concentration in parts per million volumetric	ppmv
C_i	Carbon concentration seawater	g C m^{-3}
D	Diffusion coefficient in ocean	m² y^{-1}
F_{fa}	Flux from fossil reservoir (N_f) to atmosphere (N_a)	Gt C y^{-1}
F_g	Precipitation flux of organic matter in the sea	Gt C y^{-1}
F_{ma}	Flux from oceanic mixed layers to the atmosphere (N_a)	Gt C y^{1}
$FO_{i,j}$	Flux between ocean layer i and j	Gt C y^{-1}
H_j	Carbon in humus in ecosystem j	Gt C
HDIST	Carbon flux released from biosphere by human disturbance	Gt C y^{-1}
i j	number of ocean layer (1-12) or of ecosystem	
k	Componentnumber (1= leaf, 2 = branch, 3 = stem, 4 = root)	
K_i	Carbon in charcoal and other long-living soil carbon in ecosystem j	Gt C
L_j	Carbon in litter in ecosystem j	Gt C
N_a	Carbon in atmosphere	Gt C
N_f	Carbon in fossil reservoirs	Gt C
NPP_j	Net primary production of ecosystem j	Gt C y^{-1}
NEP_j	Net Ecosystem production of ecosystem j	Gt C y^{-1}
O_i	Carbon in ocean layer i	Gt C
$O_{i,eq}$	O_i, if in equilibrium with C_a	Gt C
p_{jk}	Fraction of NPP partitioned to component k in ecosystem j	
T	Thickness of ocean layer	m
TNEP	NEP, summed over all ecosystems	Gt C y^{-1}
V_i	Volume of ocean layer i	m³
β	Biotic growth factor of CO_2 to σ(NPP)	-

ε_k	Carbonization fraction of component k upon burning	-
ε_L	Carbonization fraction of litter upon burning	-
ζ	Buffer (or Revelle) factor of CO_2 in seawater	-
λ_j	Humification fraction in ecosystem j	
$\sigma(X)$	Surface density of X	Gt C Mha^{-1}
ϕ_j	Carbonization fraction of humus in ecosystem j upon decomposition	-
$\emptyset$	Mass flow of water	m^3 y^{-1}
τ	Life-span or relaxation time	y

REFERENCES

Ajtay, G.L., P. Ketner & P. Duvigneaud, 1979. Terrestrial primary production and phytomass. In: Bolin et al. (Eds), pp. 129-187.

Bacastow, R. and C.D. Keeling, 1973. Atmospheric carbon dioxide and radio carbon in the natural carbon cycle: II Changes from AD 1700 to 2070 as deduced from a geochemical model. In Woodwell and Pecan (Eds.). Carbon and the Biosphere. NTIS U.S. Dept. of commerce, Springfield, Virginia, AEC Symp. Ser. 30, pp. 86-135.

Björkström, A., 1979. A Model of CO_2 Interaction between Atmosphere, Oceans and Land Biota. In: Bolin et al. (Eds.) pp 403-457.

Bolin, B., E.T. Degens, S. Kempe and P. Ketner (Eds), 1979. The global carbon cycle. Scope 13. John Wiley and Sons, New York, 491 pp.

Breman, H., I.B. Cissé et M.A. Djitèye, 1982. Exploitation, degradation et desertification. pp. 378-385. In: F.W.T. Penning de Vries et M.A. Djitèye (Eds). La productivité des pâturages sahéliens. Pudoc, Wageningen.

Broecker, W.S. & T.H. Peng, 1974. Gas exchange rate between air and sea. Tellus 26(1): 21-35.

Cooper, J.P. (Ed), 1975. Photosynthesis and productivity in different environments. IBP 3. Cambridge University Press, 715 pp.

Eckholm, E.P., 1976. Losing ground. Environmental stress and World Food Prospects. Norton, New York, 223 pp.

Fraser, P.J., P. Hyson, G.I. Pearman, 1980. Global atmospheric carbon dioxide space and time variability: an analysis, with emphasis on new data, for model validition. In: Pearman (Ed), pp 49-59.

Gifford, R.M., 1980. Carbon storage by the biosphere. In: Pearman (Ed).

Gifford, R.M. , 1979. Growth and yield of CO_2-enriched wheat under water-limited conditions. Aust.J. of Plant Physiol. 6, 367-378.

Goudriaan, J. & G.L. Ajtay, 1979. The possible effects of increased CO_2 on photosynthesis. In: Bolin et al. (Eds), pp. 239-249.

Goudriaan, J & H.H. van Laar, 1978. Relations between leaf resistance, CO_2-concentration and CO_2-assimilation in maize, beans, lalang grass and sunflower. Photosynthetica 12(3):241-249.

Goudriaan, J. & H.E. de Ruiter, 1983. The effect of CO_2 enrichment in interaction with shortage of either nitrogen or phosphorus on plant growth. Accepted by Neth. J. Agric. Sci.

Keeling, C.D., 1973. The carbon dioxide cycle: reservoir models to depict the exchange of atmospheric carbon dioxide with the oceans and land plants. In: Rasool, S.I. (Ed), Chemistry of the lower atmosphere, 251-329. Plenum Press, New York.

Kohlmaier, G.H., G. Kratz, H. Bröhl and E.O. Siré, 1981. The source-sink function of the terrestrial biota within the global carbon cycle. In: W.J. Mitsch, R.W. Bosserman and J.M. Klopatek (Eds.). Energy and ecological modelling. Elseviers Sci. Publ. Comp. Amsterdam, pp. 57-68.

Kortleven, J., 1963. Kwantitatieve aspecten van humusopbouw en humusafbraak. Pudoc, Wageningen, 106 pp.

Larcher, W., 1980. Physiological Plant Ecology. Springer-Verlag, Berlin, 303 pp.

Louwerse, W., 1980. Effects of CO_2 concentration and irradiance on the stomata behaviour of maize, barley and sunflower plants in the field. Plant, Cell and Environment 3: 391-398.

MacIntyre, F., 1980. The absorption of fossil-fuel CO_2 by the ocean. Oceanologica Acta 3(4): 505-516.

Oeschger, H., U. Siegenthaler, U. Schotter & A. Gugelmann, 1975. A box diffusion model to study the carbon dioxide exchange in nature. Tellus -27- (2), 168-192.

Pearman, G.I. (Ed), 1980. Carbon dioxide and climate: Australian Research. Australian Academy of Science, Canberra, 217 pp.

Rosenberg, N.J., 1981. The increasing CO_2 concentration in the atmosphere and its implication on agricultural productivity. Climatic Change 3, 256-279.

Seiler, W. & P.J. Crutzen, 1980. Estimates of gross and net fluxes of carbon between the biosphere and the atmosphere from biomass burning. Climatic Change 2, 207-247.

Siré, E.O., G.H. Kohlmaier, G. Kratz, U. Fischbach and H. Bröhl, 1981. Comparative dynamics of atmosphere-ocean models within the description of the perturbed global carbon cycle. Z. Naturforsch. 36a:233-250.

United Nations, 1977. Desertification: its causes and consequences. Pergamon Press, New York.

Viecelli, J.A., H.W. Ellsaesser and J.E. Burt, 1981. A carbon cycle model with latitude dependence. Climatic Change 3, 281-302.

Legends

Fig. 1. The annual release of carbon to the atmosphere by combustion of fossil fuel. The dots are historic data, which are approximated by the solid line for model purposes. Two future trends are compared in the model (dashed lines).

Fig. 2. Used stratification of the ocean, with an indication of model circulation of water.

Fig. 3. Dependence of the buffer factor ξ on the CO_2 partial pressure, expressed in ppmv.

Fig. 4. Simulated equilibrium carbon content of ocean water as a function of depth.

Fig. 5. Measured and simulated CO_2-contents of the atmosphere in ppmv, with two different models.

Fig. 6. Long term behaviour of three models for the same fossil carbon release.

Fig. 7. General structure of carbon flow through a terrestrial ecosystem.

Fig. 8. Simulated pools and fluxes of the global carbon cycle in 1980 A.D. Area of pools and width of fluxes are proportional to their sizes.

Fig. 9. Simulated pools and fluxes of the terrestrial biospheric section of the global carbon cycle in 1980 A.D.

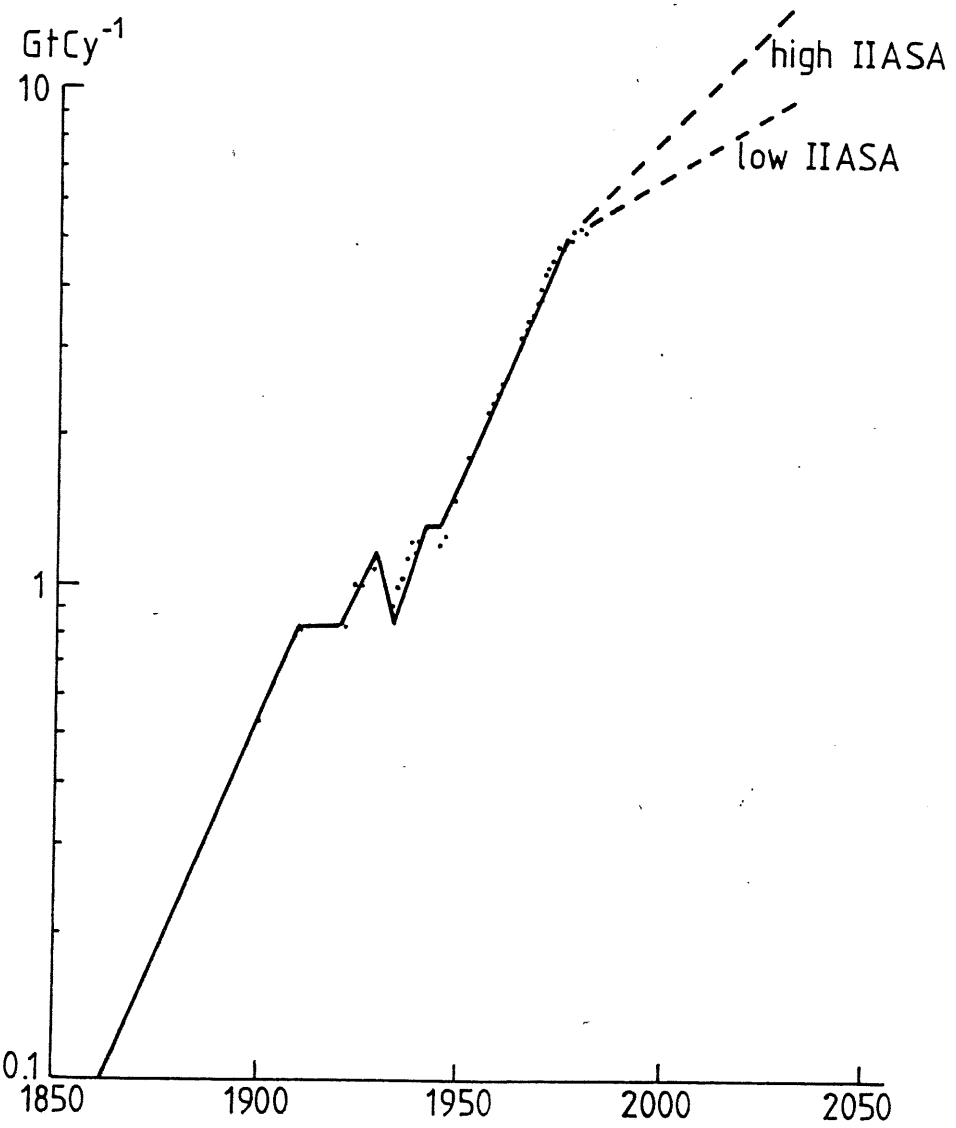

Fig 1

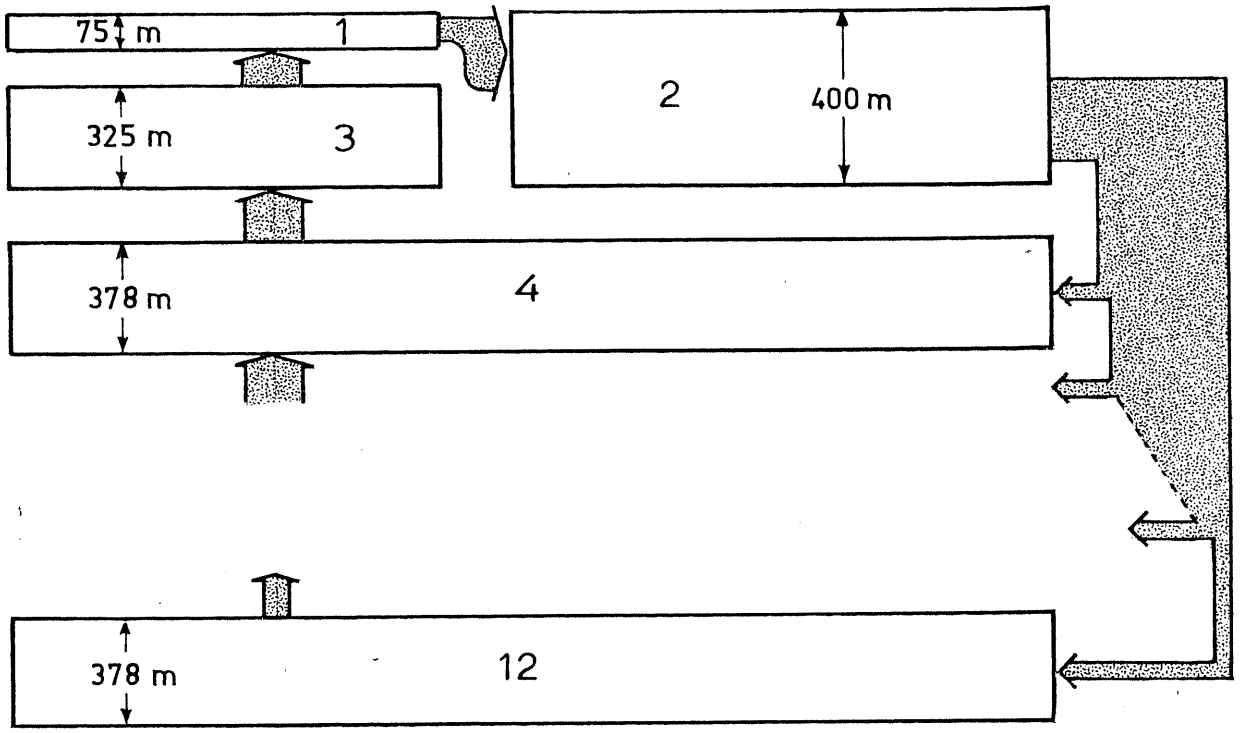

Fig 2

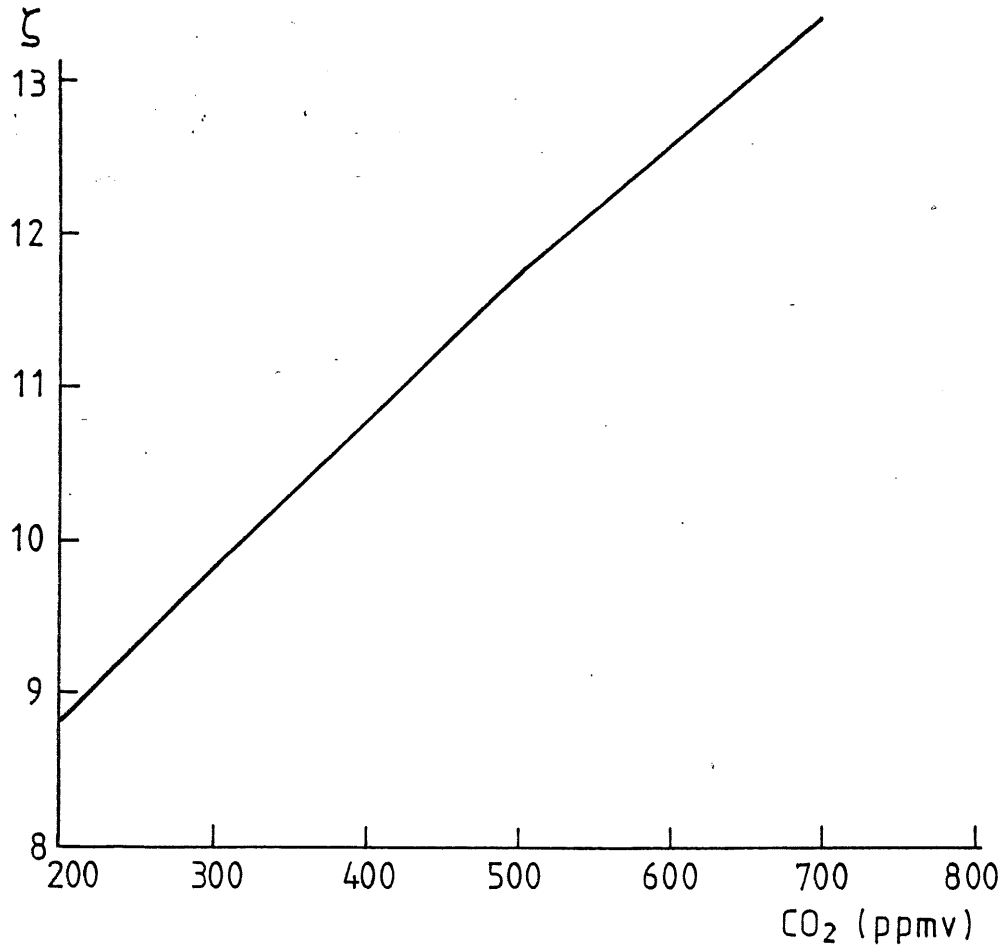

Fig 3

Fig 4

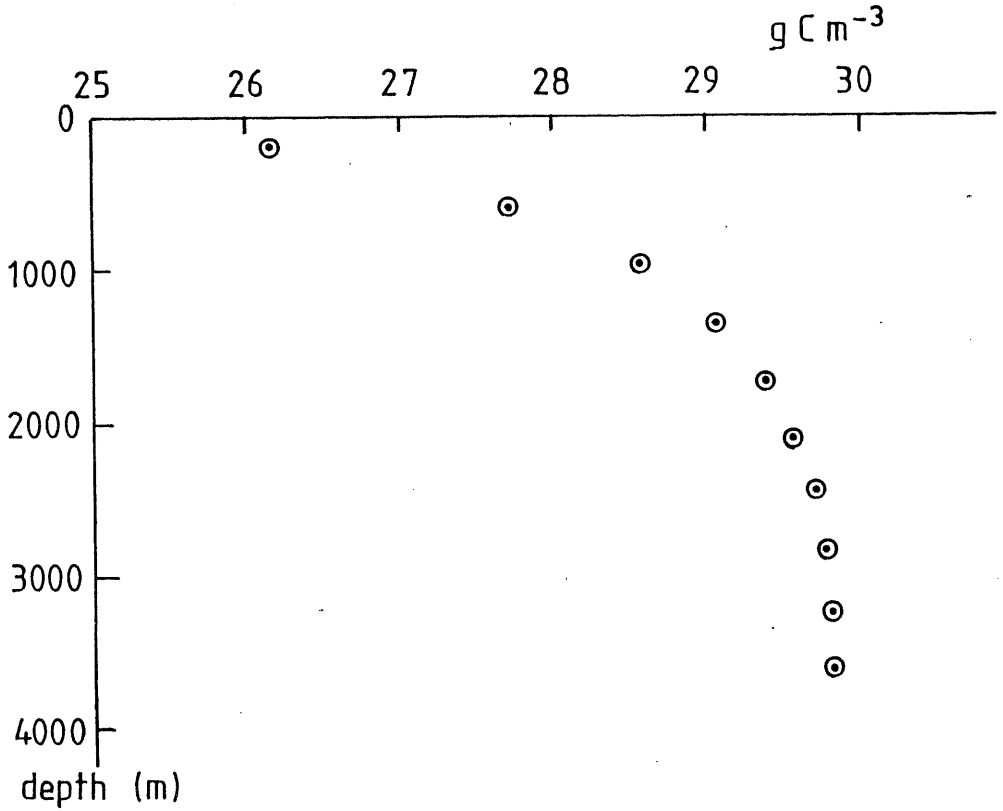

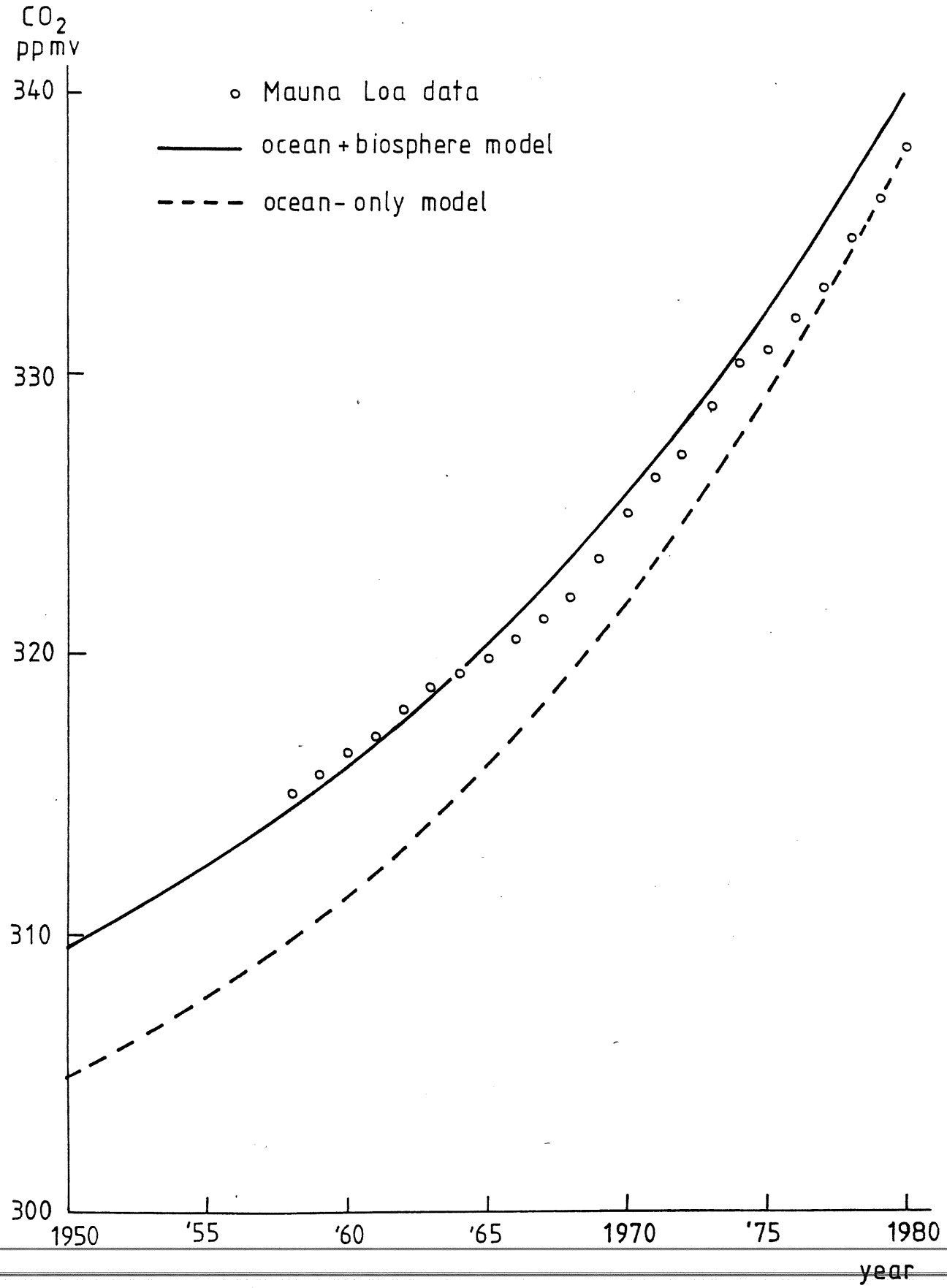
CO_2
ppmv
340
330
320
310
300
o Mauna Loa data
ocean + biosphere model
ocean - only model
1950
'55
'60
'65
1970
'75
1980
year

Fig 5

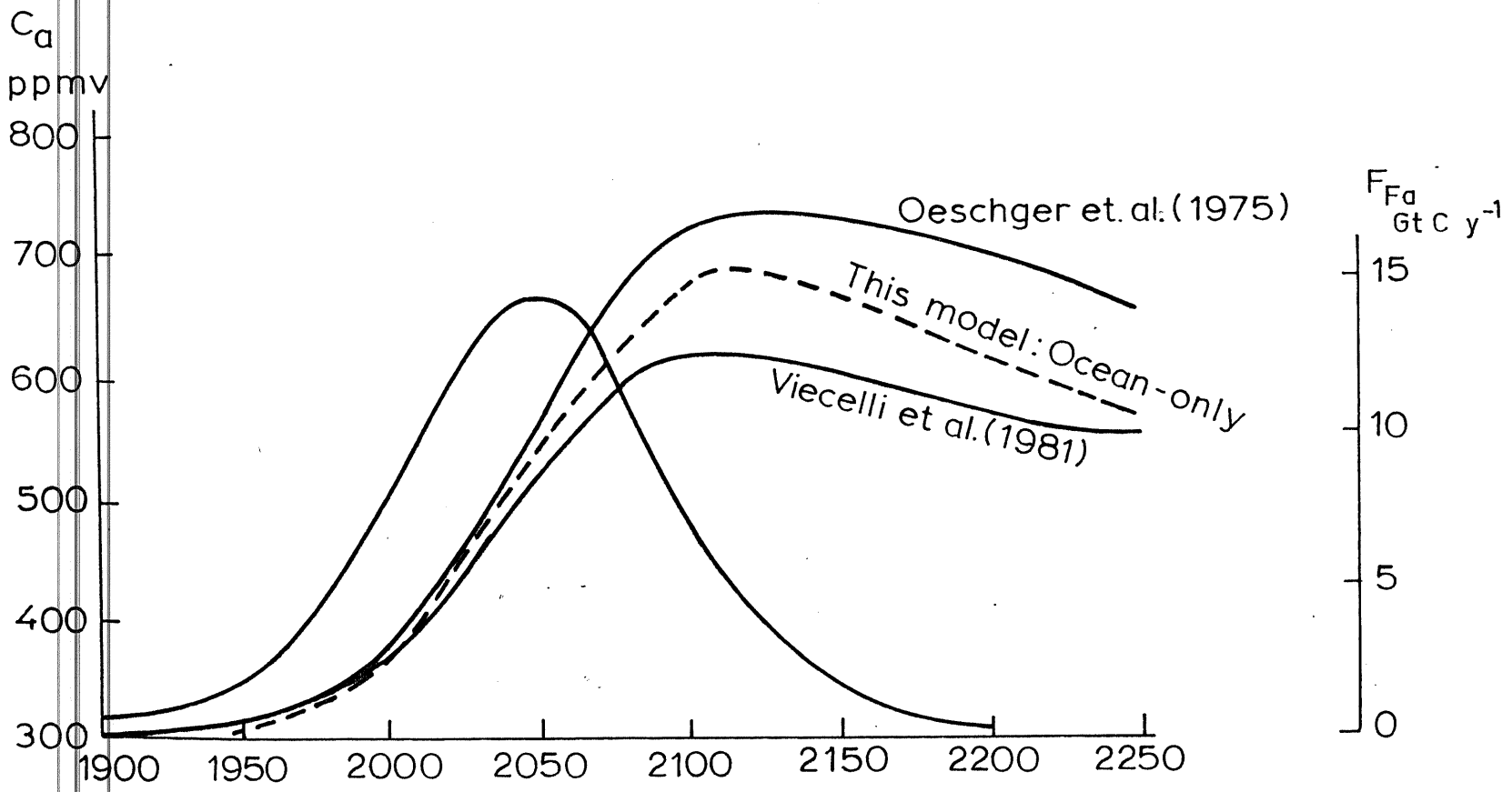
C_a
ppmv
800
700
600
500
400
300
1900
1950
2000
2050
2100
2150
2200
2250
Oeschger et. al. (1975)
This model: Ocean-only
Viecelli et al. (1981)
F_{Fa}
Gt C y^{-1}
15
10
5
0

Fig 6.

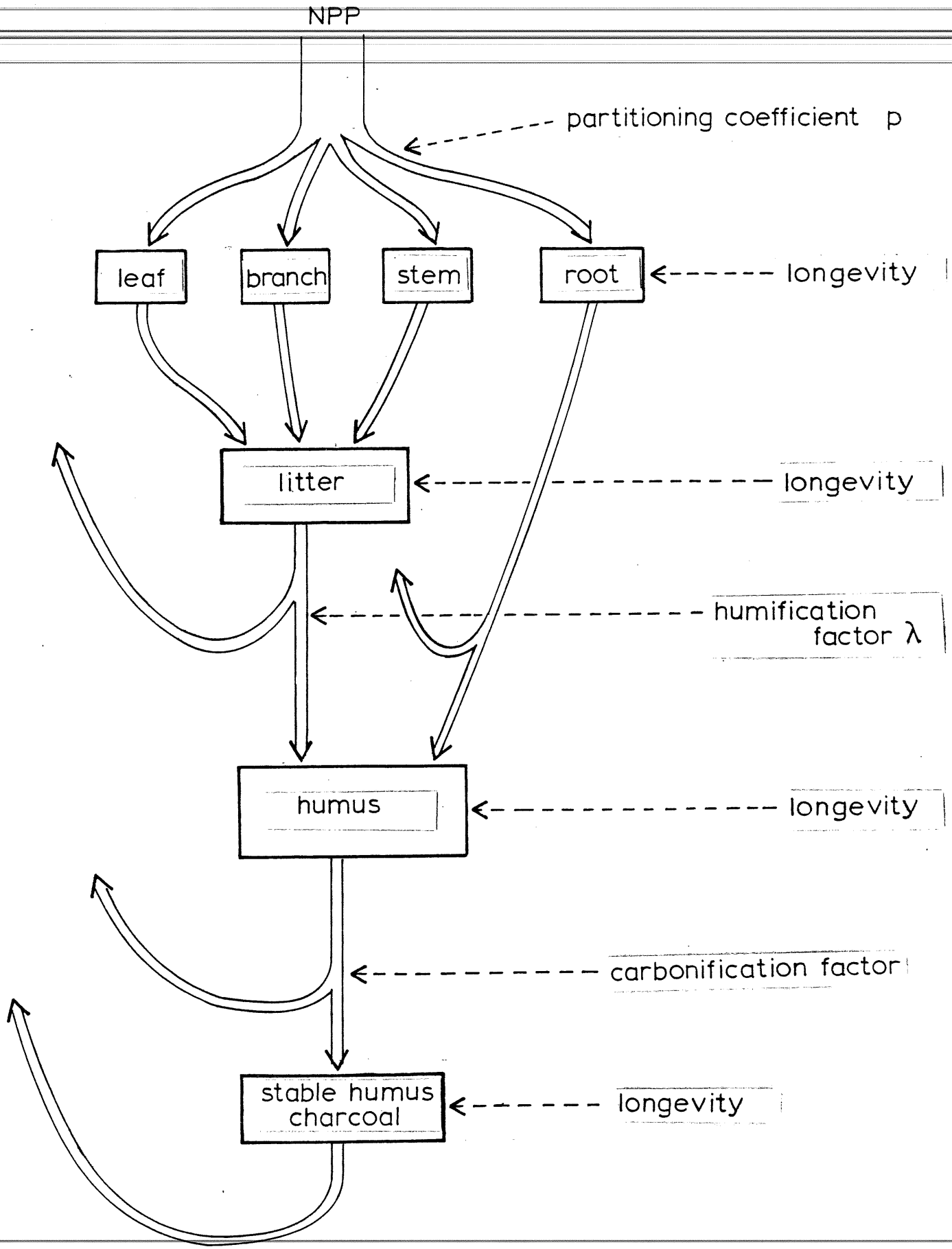
NPP
partitioning coefficient p
leaf
branch
stem
root
longevity
litter
longevity
humification factor λ
humus
longevity
carbonification factor
stable humus charcoal
longevity

Fig 7

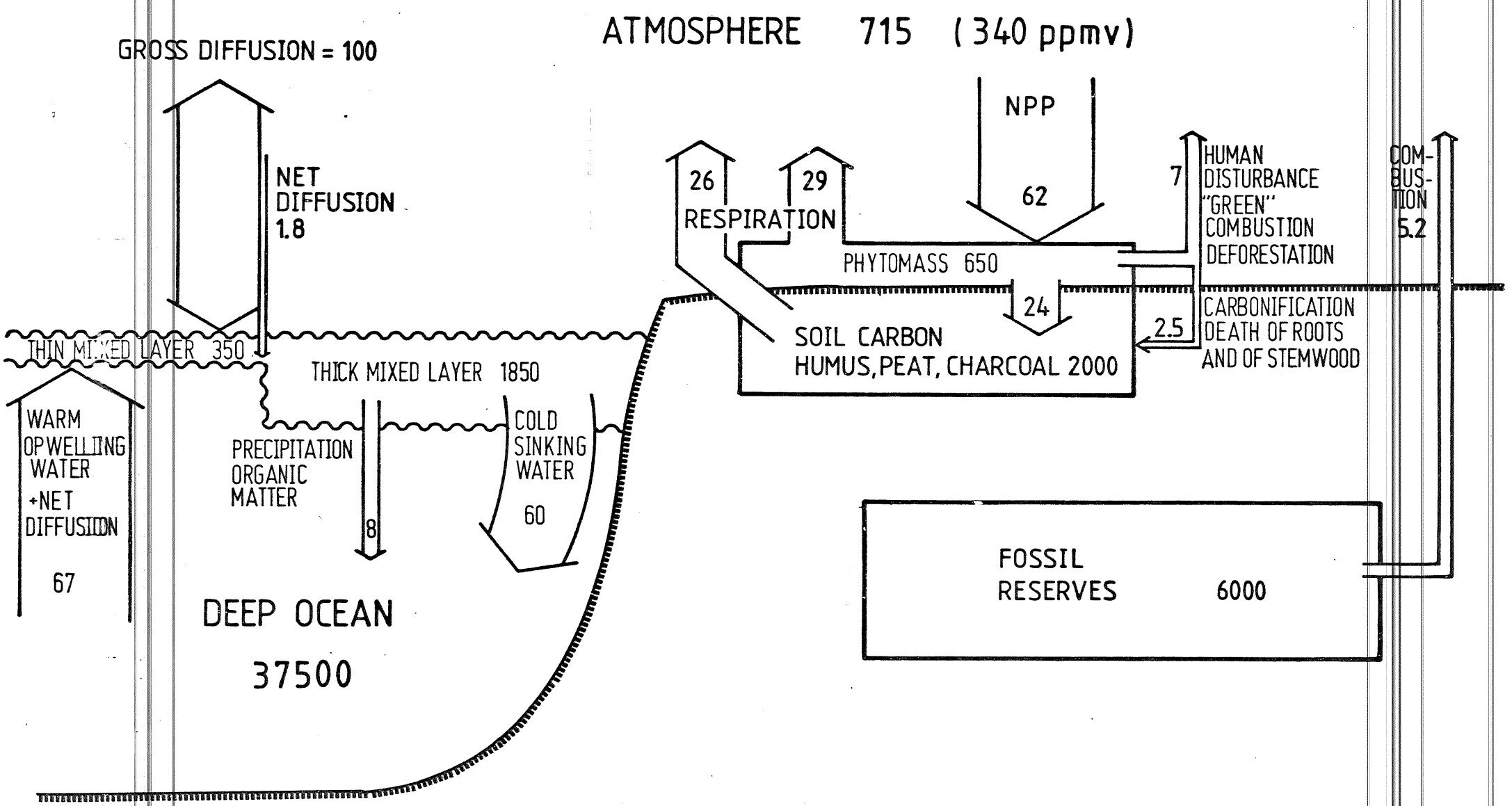
ATMOSPHERE 715 (340 ppmv)
GROSS DIFFUSION = 100
NET DIFFUSION 1.8
NPP
62
26
RESPIRATION
29
7
HUMAN DISTURBANCE "GREEN" COMBUSTION DEFORESTATION
COM-BUS-TION 5.2
PHYTOMASS 650
24
2.5
CARBONIFICATION DEATH OF ROOTS AND OF STEMWOOD
SOIL CARBON HUMUS, PEAT, CHARCOAL 2000
THIN MIXED LAYER 350
THICK MIXED LAYER 1850
WARM UPWELLING WATER +NET DIFFUSION
67
PRECIPITATION ORGANIC MATTER
8
COLD SINKING WATER
60
FOSSIL RESERVES 6000
DEEP OCEAN
37500

Fig 8

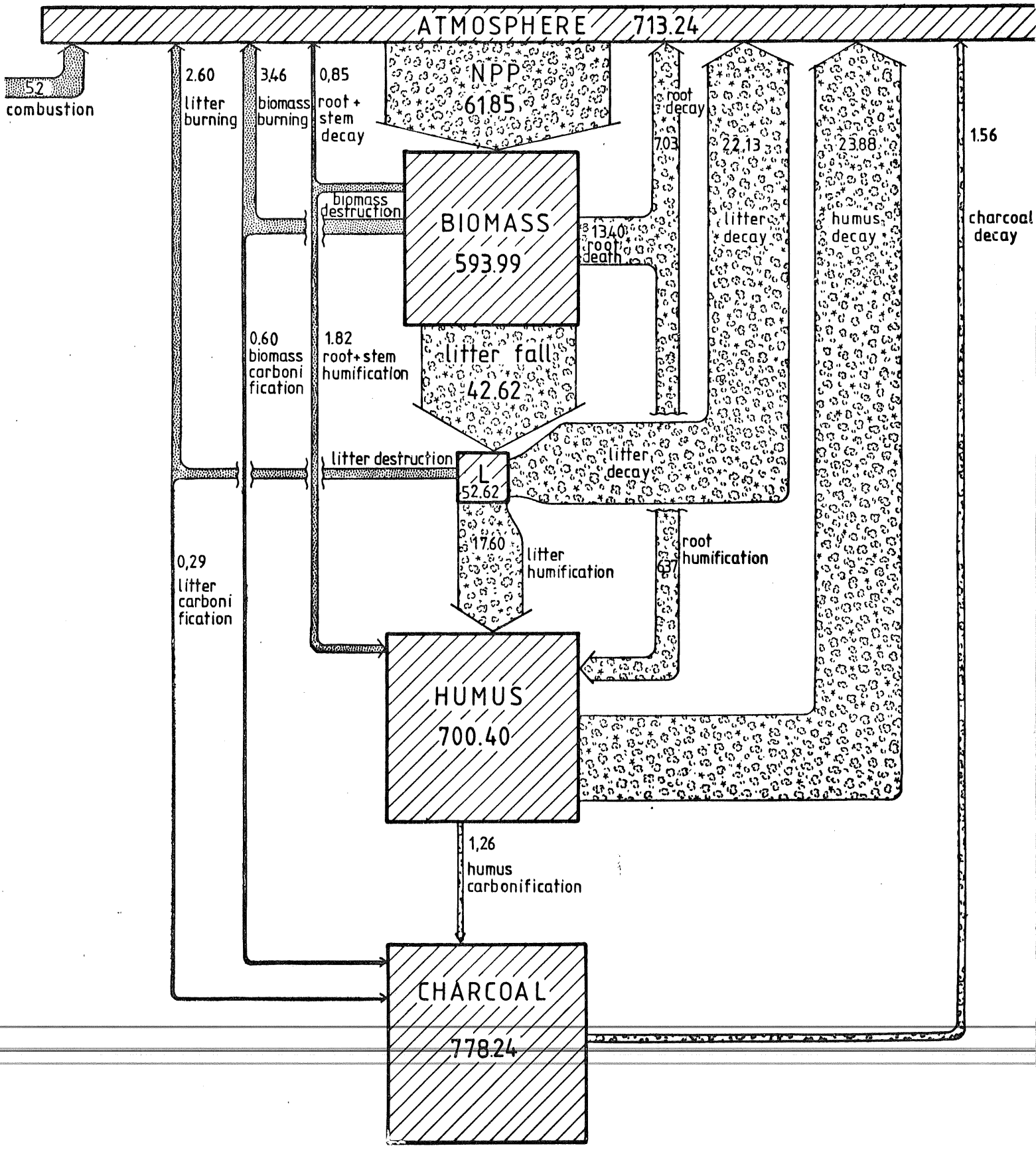
ATMOSPHERE 713.24
5.2
combustion
2.60
litter
burning
3.46
biomass
burning
0,85
root +
stem
decay
NPP
6185
root
decay
7.03
22.13
litter
decay
23.88
humus
decay
1.56
charcoal
decay
biomass
destruction
BIOMASS
593.99
13.40
root
death
0.60
biomass
carboni
fication
1.82
root+stem
humification
litter fall
42.62
litter destruction
L
52.62
litter
decay
17.60
litter
humification
.37
root
humification
0,29
litter
carboni
fication
HUMUS
700.40
1,26
humus
carbonification
CHARCOAL
778.24

Fig 9